Biomechanical Analysis of the Personalized Vehicle

Project AMF-V1-1176

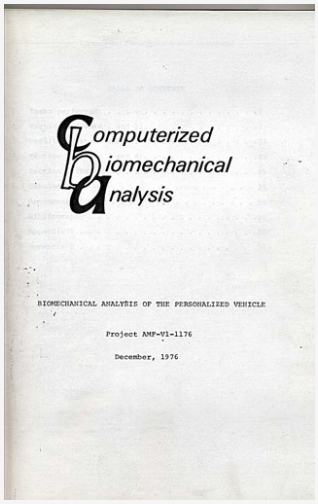

Code	**adi-pub-01201**
Title	Biomechanical Analysis of the Personalized Vehicle
Subtitle	Project AMF-V1-1176
Name	Computerized Biomechanical Analysis Inc.
Author	Gideon Ariel
Published on	Wednesday, December 1, 1976
Subject	Journal; Science
URL	https://arielweb.com/articles/show/adi-pub-01201
Date	2013-01-16 15:40:49
Label	Approved
Privacy	Public

Below find a reprint of the 39 relevant pages of the article "Biomechanical Analysis of the Personalized Vehicle" in "Computerized Biomechanical Analysis Inc.":

Computerized Biomechanical Analysis

BIOMECHANICAL ANALYSIS OF THE PERSONALIZED VEHICLE

Project AMF-V1-1176

December, 1976

TABLE OF CONTENTS

1. Tasks performed. 1
2. Section 1 (Tasks 1 and 2). 2
3. Results (Tasks 1 and 2). 11
4. Section 2 (Tasks 3 and 4). 22
5. Section 3 (Task 5) 24
6. Conclusions 25
7. Recommendations 28
Bibliography 29
Appendix 1 30
Appendix 2 31

Project AMF-V1-1176
December, 1976

BIOMECHANICAL ANALYSIS OF THE PERSONALIZED VEHICLE

The project consisted of the tasks outlined below:

1. Evaluate the deceleration patterns for stopping or braking the vehicle. The kinematic parameters for the most abrupt stop that could be generated were determined on two riders, one adult (male) and one child (male) who propelled the vehicle at maximum possible manual speed.

2. Perform a kinematic analysis on both the adult and the child utilizing cinematography. Perform kinetic analyses on the same subjects from the kinematic results and from a knowledge of the external forces on the subjects. Utilize force plates to provide exact force magnitudes for various styles and rates of body motion used in propelling the vehicle.

3. Determine the energy cost analysis based on the impulse and its correlation with heart rate for both the adult and child riders.

4. Compare the heart rate for propelling the vehicle with that for running at approximately the same speed.

5. Determine the induced body forces when traversing road obstacles (bumps) and evaluate them as a potential for bodily damage.

SECTION 1 (TASKS 1 and 2)

EXPERIMENTAL PROCEDURES

The experimental procedures included two data collection processes:

1. Cinematographical data

2. Force platform data

Cinematographical Data Collection

Data was collected on riders performing in both normal mode and braking mode. The rider followed a straight path and the cameras, side and rear, started when the rider reached a particular location. For the braking test, the rider was instructed to apply the brakes at a predetermined point. Ten trials were filmed in each of the two modes. Figures 1 and 2 illustrate a normal mode trial from the side and rear respectively.

High speed cinematography (at rates from 64 to 100 frames per second) was used to record the motion of the subjects riding the vehicle. This technique permitted an accurate recording of the individuals' performances under actual conditions.

Cinematographical data were used in conjunction with data collected from the force platforms. The measured forces were synchronized with the cinematographical information and applied (by computer simulation) as external forces for determination of body kinetic forces.

Figure 1 Normal setup side view

Figure 2 Normal setup rear view

Force Platform Data Collection

Two force platforms were used in the laboratory to record the three orthogonal forces at the wheels (lateral, horizontal, and vertical). Cinematographic data were obtained simultaneously in order to provide information as to the pattern of motion of the vehicle. Figures 3 and 4 illustrate the laboratory experimental arrangement.

The forces exerted by the rear and front wheels during movement were analyzed. As the vehicle progressed across the force plate, the instantaneous vertical, horizontal, and lateral components of force were obtained. These components were converted into analog electrical signals and displayed on a storage oscilloscope. The force data was simultaneously sampled at a high rate by a Biomation unit which converted the analog data into digital values. The digital information was transmitted to a computer and stored for subsequent processing. Figure 4A is a schematic of the signal processing that takes place. Figure 5 illustrates a typical lateral force curve.

Calculation of Forces --- Cinematographical Method

A composite tracing of the joint centers of the body was obtained by single frame projection of the film on a digitizer screen. The model GP-3 Graf-Pen digitizer was used for determination of the coordinates of the joint centers. These X

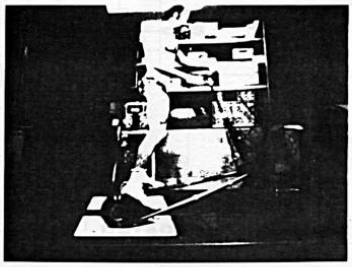

Figure 3 Laboratory setup side view

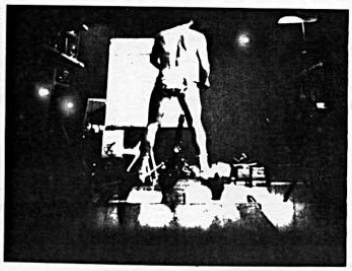

Figure 4 Laboratory setup rear view

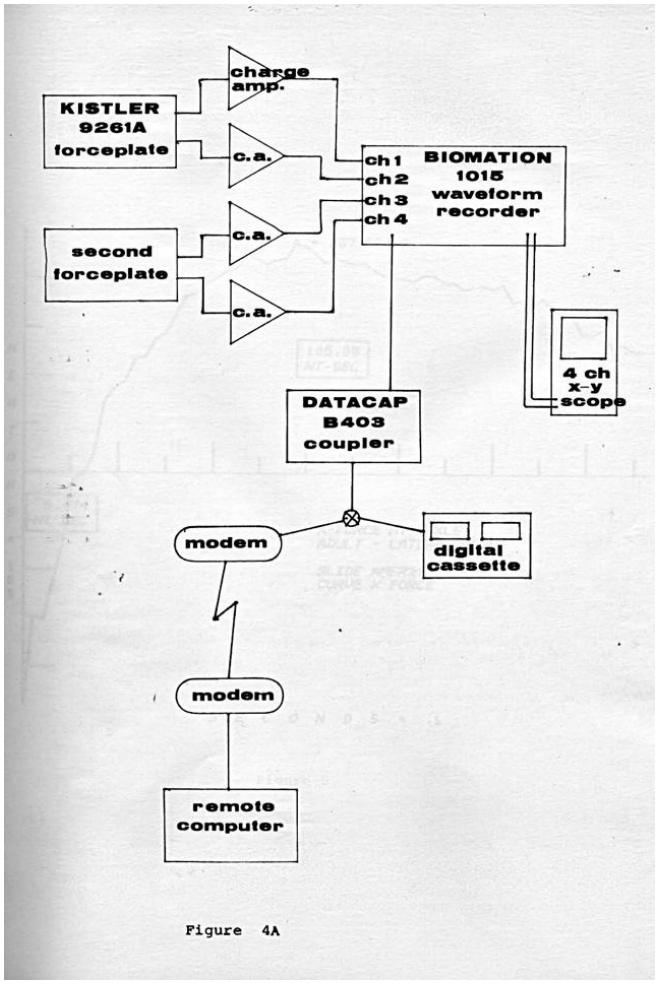

Figure 4A

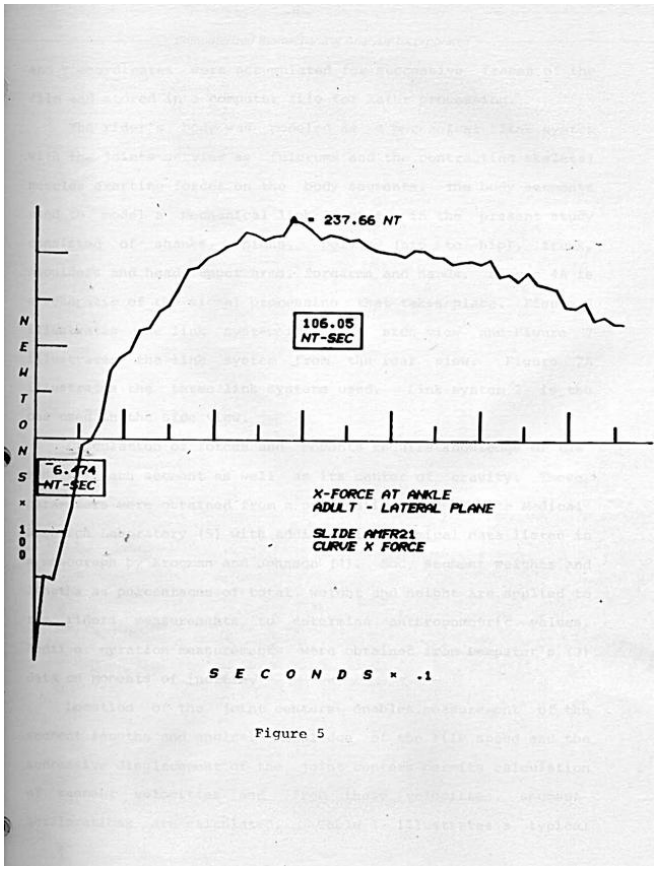

Figure 5

and Y coordinates were accumulated for successive frames of the film and stored in a computer file for later processing.

The rider's body was modeled as a mechanical link system with the joints serving as fulcrums and the contracting skeletal muscles exerting forces on the body segments. The body segments used to model a mechanical link system in the present study consisted of shanks, thighs, pelvis (hip to hip), trunk, shoulders and head, upper arms, forearms and hands. Figure 4A is a schematic of the signal processing that takes place. Figure 6 illustrates the link system from the side view and Figure 7 illustrates the link system from the rear view. Figure 7A illustrates the three link systems used. Link system 2 is the one used in the side view.

Calculation of forces and moments require knowledge of the mass of each segment as well as its center of gravity. These parameters were obtained from a publication by Aerospace Medical Research Laboratory (5) with additional anatomical data listed in a monograph by Krogman and Johnson (4). Body segment weights and lengths as percentages of total weight and height are applied to the riders measurements to determine anthropometric values. Radii of gyration measurements were obtained from Dempster's (3) data on moments of inertia.

Location of the joint centers enables measurement of the segment lengths and angles. Knowledge of the film speed and the successive displacement of the joint centers permits calculation of segment velocities and from these velocities, segment accelerations are calculated. Table 1 illustrates a typical

One link system

1 - Shank
2 - Thigh
3 - Trunk
4 - Upperarm
5 - Forearm

Figure 6 Side view link system

Link No. 1

1 - R-Shank
2 - R-Thigh
3 - Hip to Hip
4 - L-Thigh
5 - L-Shank

Link No. 2

1 - R-Shank
2 - R-Thigh
6 - Hip to Shoulder
7 - R-Upperarm
8 - R-Forearm

Primary Link

1 - R-Shank
2 - R-Thigh
6 - Hip to Shoulder
9 - Accross Shoulders
10- L-Upperarm
11- L-Forearm

Figure 7 Two secondary and primary link systems from rear view.

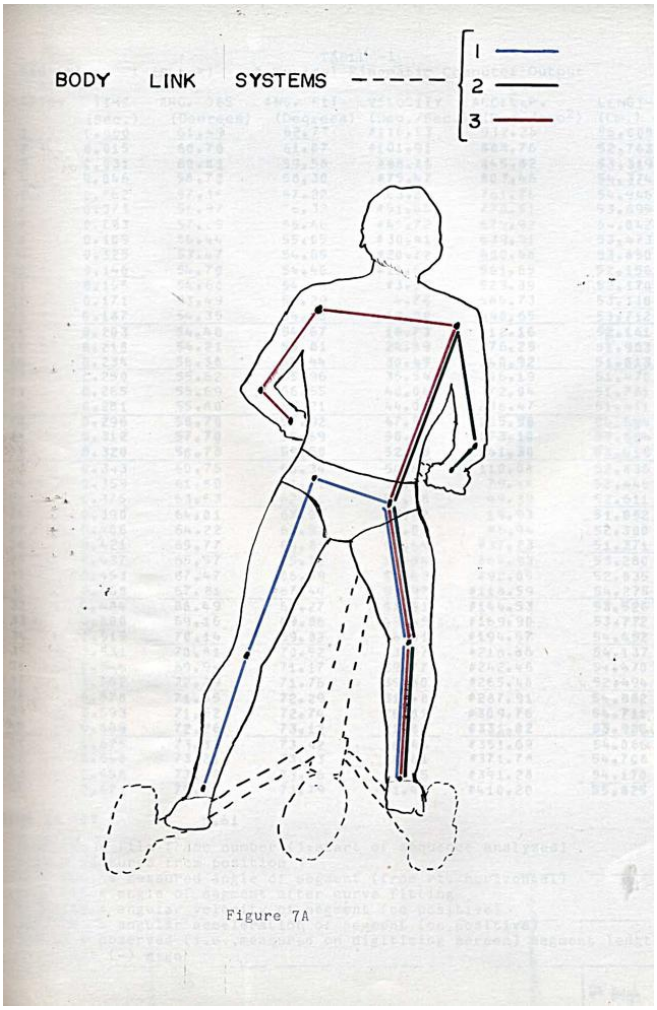

Figure 7A

TABLE -1

SEGMENT 1 (Shank) A Typical Kinematic Computer Output

POSITION	TIME (Sec.)	ANG. OBS (Degrees)	ANG. FIT (Degrees)	VELOCITY (Deg./Sec.)	ACCELER. (Deg./sec^2)	LENGTH (Cm.)
1	0.000	61.49	62.77	#116.13	932.26	56.008
2	0.015	60.70	61.07	#101.91	884.76	52.763
3	0.031	60.01	59.58	#88.35	845.82	53.319
4	0.046	58.72	58.30	#75.47	803.46	54.374
5	0.062	57.35	57.22	#63.24	761.70	54.946
6	0.078	56.97	56.32	#51.66	720.51	53.695
7	0.093	57.15	55.60	#40.72	679.92	54.042
8	0.109	56.44	55.05	#30.41	639.91	53.473
9	0.125	53.47	54.65	#20.72	600.48	53.850
10	0.140	54.70	54.40	#11.65	561.65	52.156
11	0.156	54.60	54.28	#3.17	523.39	52.170
12	0.171	53.49	54.29	4.70	485.73	53.110
13	0.187	54.35	54.43	12.00	448.65	53.712
14	0.203	54.40	54.67	18.73	412.16	52.141
15	0.218	54.21	55.01	24.89	376.25	51.963
16	0.234	56.38	55.44	30.49	340.92	51.813
17	0.250	55.62	55.96	35.54	306.19	51.470
18	0.265	55.69	56.55	40.06	272.04	51.781
19	0.281	55.80	57.21	44.05	238.47	51.411
20	0.296	56.70	57.92	47.52	205.50	54.604
21	0.312	57.70	58.69	50.47	173.10	53.604
22	0.328	58.78	59.50	52.93	141.30	53.419
23	0.343	60.75	60.34	54.89	110.08	52.836
24	0.359	61.80	61.21	56.37	79.44	52.446
25	0.375	63.63	62.10	57.38	49.39	52.611
26	0.390	64.01	63.00	57.92	19.93	51.052
27	0.406	64.22	63.91	58.00	#8.94	52.300
28	0.421	65.77	64.81	57.64	#37.23	51.371
29	0.437	65.57	65.71	56.84	#64.93	53.280
30	0.453	67.47	66.59	55.62	#92.05	52.835
31	0.468	67.81	67.44	53.97	#118.59	54.275
32	0.484	68.49	68.27	51.91	#144.53	53.526
33	0.500	69.16	69.06	49.45	#169.90	53.772
34	0.515	70.14	69.82	46.61	#194.67	54.452
35	0.531	70.81	70.52	43.37	#218.86	54.137
36	0.546	69.90	71.17	39.77	#242.46	54.470
37	0.562	72.29	71.76	35.80	#265.48	52.494
38	0.578	71.35	72.29	31.48	#287.91	54.882
39	0.593	71.62	72.74	26.81	#309.76	54.711
40	0.609	72.26	73.12	21.80	#331.02	53.900
41	0.625	73.33	73.42	16.46	#351.69	54.066
42	0.640	73.21	73.63	10.81	#371.78	54.708
43	0.656	73.27	73.76	4.85	#391.28	54.170
44	0.671	75.81	73.79	#1.40	#410.20	55.825

ERROR IN FIT 5.61

Position = film frame number (1=start of sequence analyzed)
time = measured from position 1
Ang. Obs. = measured angle of segment (from rt. horizontal)
Ang. fit = angle of segment after curve fitting
velocity = angular velocity of segment (cc positive)
acceler. = angular acceleration of segment (cc positive)
length = observed (i.e.,measured on digitizing screen) segment length
# = minus (-) sign

cinematographical kinematic computer output.

From the kinematic data, and from calculation of centers of gravity, radii of gyration, and segment masses, the segment forces and moments were determined. Appropriate programming resulted in a segment by segment analysis of body motion, including the total body center of gravity; segment velocities and accelerations; horizontal, vertical, and resultant forces; angle of the resultant force application; moments (indicative of the magnitude of the muscle action at each joint); vertical and horizontal forces at the ground contact points; timing or coordination of motion between the body segments; and the relative motion between the body segments. Table 2 illustrates a computer output of a typical kinetic analysis. Appendix 1 presents a total kinematic and kinetic output.

To obtain the forces due to motion of the body segments used in the present study, the body was treated as three link systems---one primary and two secondary. Each link system must consist of a continuous series of body segments, without repetition, beginning at a fixed point (in the present study, one ankle joint was selected as the fixed point). The entire body cannot be expressed as a single link system since there are two joints (hip and shoulder) where three segments intersect. Any continuous series of segments through these joints can include, at most, two of the segments. The third segment is accounted for by including it in a secondary link system (two of these are necessary to accomodate the two joints in question). The forces calculated for these secondary link systems are then

CHILD - SIDE WT W - BRAKING - AMFS71

DEC. 15, 1976 - EXTERNAL FORCES APPLIED

TABLE 2

Typical Kinetic Computer Output

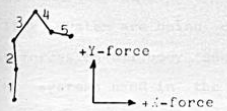

Force = Resultant

PHI = angle (from x - axis)

= minus (-) sign

LINK SYSTEM NUMBER 1

POSITION 1 (Forces in Grams; Moment in Gram-Cm)

SEGMENT	X FORCE	Y FORCE	FORCE	PHI	MOMENT
1	#15482.50	#9905.45	18380.04	212.610	#918855.
2	#15148.09	#7703.89	16994.55	207.956	#508537.
3	#13159.42	#4391.20	17872.74	198.453	#109112.
4	#10367.07	#104.09	10367.59	180.575	235222.
5	#9639.35	1061.50	9697.62	173.715	75616.

POSITION 2

SEGMENT	X FORCE	Y FORCE	FORCE	PHI	MOMENT
1	#15371.43	#10236.12	18467.78	213.660	#946027.
2	#15051.80	#8007.72	17049.35	208.013	#517936.
3	#13137.05	#4564.80	13907.54	199.161	#92837.
4	#10413.35	#113.66	10414.03	180.652	247617.
5	#9698.73	1072.14	9755.82	173.690	86606.

POSITION 3

SEGMENT	X FORCE	Y FORCE	FORCE	PHI	MOMENT
1	#14811.46	#10580.81	18202.55	215.547	#895838.
2	#14528.67	#8320.42	16742.51	209.739	#494941.
3	#12809.82	#4771.63	13655.76	200.272	#75400.
4	#10335.37	#112.40	10335.98	180.623	245975.
5	#9673.75	1108.83	9737.09	173.461	82902.

POSITION 4

SEGMENT	X FORCE	Y FORCE	FORCE	PHI	MOMENT
1	#14351.63	#10843.56	17987.56	217.073	#854256.
2	#14098.43	#8559.56	16493.39	211.263	#469050.
3	#12540.05	#4864.21	13450.40	201.200	#51347.
4	#10269.12	#123.27	10269.86	180.687	257827.
5	#9652.53	1114.23	9717.08	173.391	96112.

POSITION 5

SEGMENT	X FORCE	Y FORCE	FORCE	PHI	MOMENT
1	#13485.27	#10993.33	17310.29	216.369	#822519.
2	#13653.83	#8132.44	16185.97	212.482	#442546.
3	#12238.74	#4926.41	13192.66	201.922	#45128.
4	#10169.74	#110.17	10170.33	180.620	262701.
5	#9600.70	1140.70	9668.23	173.224	92798.

POSITION 6

SEGMENT	X FORCE	Y FORCE	FORCE	PHI	MOMENT

applied at the two "three-way" joints when the forces for the primary link system are being calculated. This yields the net resultant forces on all body segments. Figure 7 illustrates the three link systems used in the present study. The computer program utilized the following procedures to calculate body forces (see schematic on following page):

1. Kinetic analysis of link system number 1 with force plate data (from the rear wheel) applied as an external force at the foot not selected as the fixed point. The forces at the hip joint were saved for later application to the primary link system as external forces.
2. Kinetic analysis of link system number 2 with force plate data (from the front wheel) applied as an external force to the hand. The forces computed at the shoulder joint were saved for later application as external forces on the primary link system.
3. Kinetic analysis of link system number 3, with force plate data (from the front wheel) applied to the hand, and with external forces from link systems 1 and 2 applied at the hip and shoulder respectively. Resultant forces computed for this link system represent total body resultant forces.

Determination of Force-Motion Relationships

LINK SYSTEMS AND EXTERNAL FORCES
FOR TOTAL BODY ANALYSIS

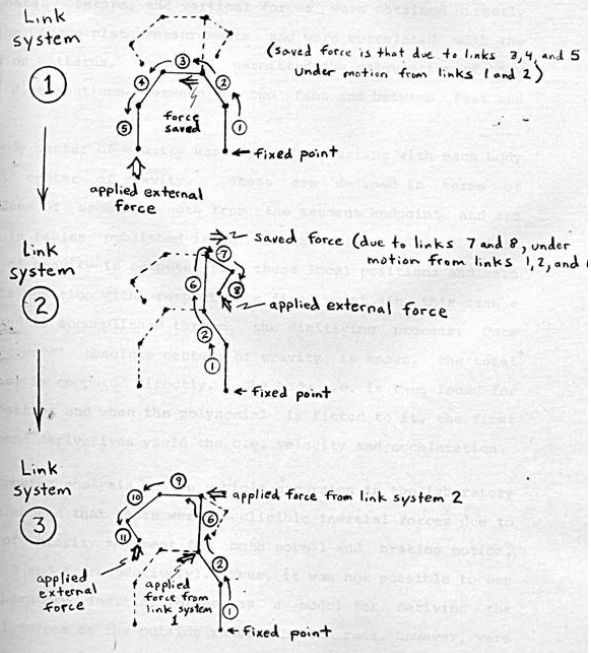

The data obtained in the laboratory enabled simultaneous calculations of forces from the cinematographical and the force plate data. Lateral and vertical forces were obtained directly from the force plate measurements and were correlated with the excursion patterns. This data permitted the calculation of body weight distributions between the two feet and between feet and hands.

Body center of gravity was found by starting with each body segment center of gravity. These are defined in terms of percentage of segment length from the segment endpoint and are found in tables published in a NASA study(4). The absolute center of gravity is computed from these local positions and each segments position with respect to a fixed point (in this case a foot) and is accomplished through the digitizing process. Once each segments' absolute center of gravity is known, the total body c.g. is computed directly. The body c.g. is thus found for each position and when the polynomial is fitted to it, the first and second derivatives yield the c.g. velocity and acceleration.

Computer analysis of the vehicle excursion in the laboratory setting showed that there were negligible inertial forces due to center of gravity movement for both normal and braking motion, (Tables 3 and 4, respectively). Thus, it was not possible to use the laboratory inertial forces as a model for deriving the inertial forces on the outside runs. The lab runs, however, were also a test of the validity of the approach and programming. By analyzing a side view and placing one force plate under the front wheel and one under the rear wheel closest to the camera, the

program output could be corraborated. The kinetic motion was analyzed by applying the forces recorded at the front plate as external force inputs to the kinetic program. The output from the program was then compared to the actual forces recorded on the rear plate. Figure 7B shows the force plate output and the computed output. The initial spike on the force platform curve was due to the wheel bumping against its edge.

Thus the displacement, velocity, and acceleration of the center of gravity were used from the outside cinematographical analyses, along with computed vehicular velocities and accelerations, to arrive at the vehicle reaction forces on the rider for each trial. Coriolis forces for the rider and vehicle relative to the ground were assumed small and therefore not included. The kinetic program computations, however, do include the Coriolis forces relative to the vehicle. These reaction forces were applied in the kinetic analyses as external forces on the appropriate body segments in order to compute true dynamic body forces. The reaction forces were computed as follows:

$$F_{reaction} = m_{person}(acceleration_{vehicle} - acceleration_{c.g.})$$

since the center of gravity displacement, velocity, and acceleration were computed with respect to one of the rider's feet (determination of this fixed point was based on the portion of the excursion that the rider was in). The acceleration relation, then, was

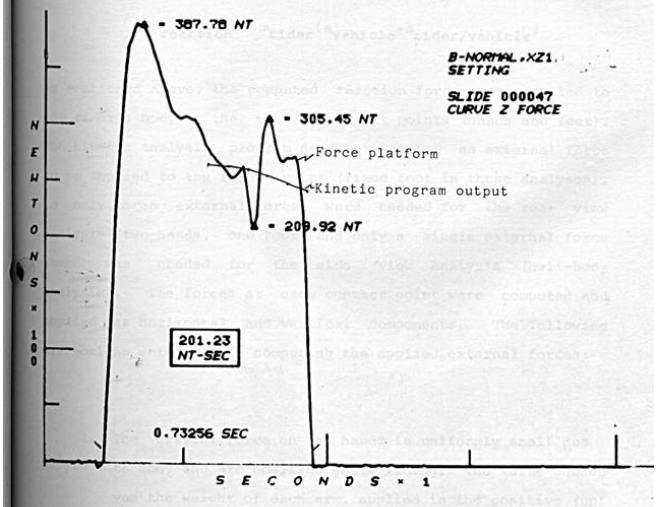

Figure 7B

$$a_{rider\ c.g.} = a_{vehicle} + a_{rider/vehicle}$$

The external force to be applied to the rider, then, was

$$F_{reaction} = m_{rider}(a_{vehicle}+a_{rider/vehicle})$$

As mentioned above, the computed reaction forces were applied to the rider's body at the vehicle contact points (hands and feet). The kinetic analysis program does not require an external force to be applied to the fixed point (fixed foot in these analyses), so only three external forces were needed for the rear view analysis (two hands, one foot) and only a single external force (hand) was needed for the side view analysis (half-body analysis). The forces at each contact point were computed and applied as horizontal and vertical components. The following assumptions were made in computing the applied external forces:

1. The vertical force on the hands is uniformly small due to body and arm position while riding. The value chosen was the weight of each arm, applied in the positive (up) direction at each hand.
2. The horizontal force on the hands in normal riding mode is small and can be ignored (if the net horizontal force on the hands were not small, the front wheel would turn or the vehicle would camber to reduce the force).

3. The horizontal force on the hands during braking mode is in the forward only direction, and can thus be ignored in the rear view analysis. For the side view analysis, the force is close to the total horizontal braking force (mass of rider times the difference between vehicle deceleration and rider's center of gravity deceleration with respect to the vehicle). For the one-side body analysis, one-half of this force was applied.
4. The vertical force on the second foot (not the fixed foot) for the rear view analysis is close to the body weight less the arm weights (applied to the hands disregarding variation in arm position) times the center of gravity percentage of distribution on that foot (from kinematic analysis). Although disregarding arm position biases the actual c.g., it is less than 6%.
5. The horizontal force on the non fixed foot (rear view analysis) in normal riding mode is equivalent to the mass of the rider less the mass of the arms (already applied to the hands) times the center of gravity distribution percentage times the difference between the horizontal vehicle acceleration and the rider's horizontal center of gravity acceleration. The horizontal vehicle acceleration is the radial acceleration of the vehicle while executing a half-

excursion, and is expressed by the square of the vehicular velocity divided by the radius of curvature of the half-excursion.

RESULTS

Vehicle and Rider Center of Gravity

The physical parameters measured were:

Adult vehicle

Weight = 100 newtons = 22.5 pounds

Stance Width = 55 cm = 21.7 inches

Child vehicle

Weight = 105 newtons = 23.6 pounds

Stance width = 44 cm = 17.3 inches

For the tests analyzed, the following excursion parameters were computed (see figure 7C):

Adult

Excursion radius = 427 cm = 14 feet

half-period = .83 seconds

amplitude = 85 cm = 2.8 feet

Child

Excursion radius = 448 cm = 14.7 feet

half-period = .50 seconds

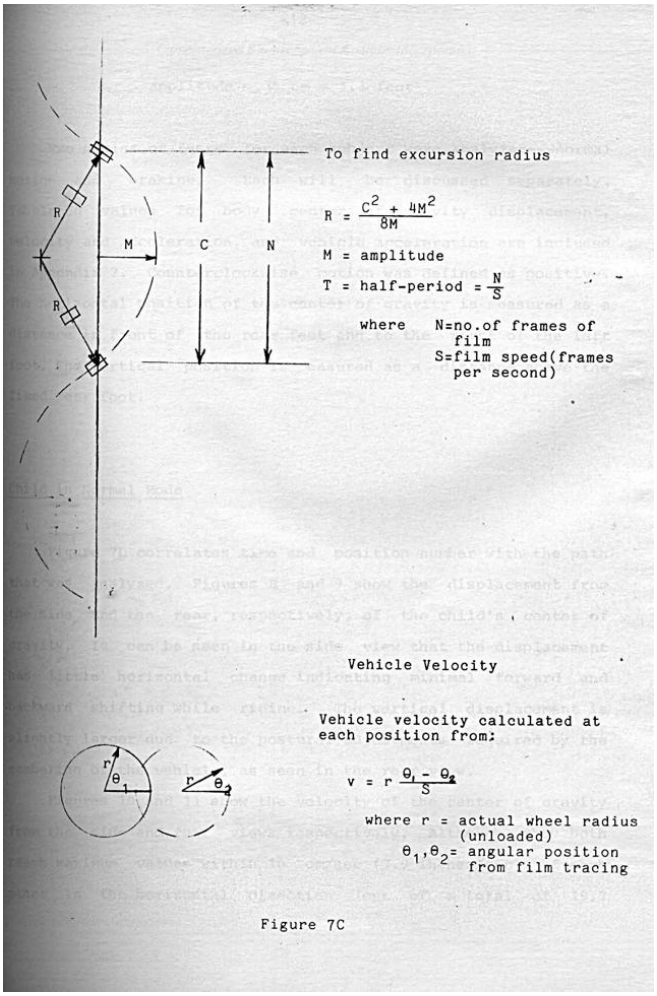

Figure 7C

amplitude = 35 cm = 1.1 feet

Two series of tests for each subject were analyzed---normal motion and braking. Each will be discussed separately. Tabulated values for body center of gravity displacement, velocity and acceleration, and vehicle acceleration are included in Appendix 2. Counterclockwise motion was defined as positive. The horizontal position of the center of gravity is measured as a distance in front of the rear feet and to the right of the left foot. The vertical position is measured as a distance above the fixed rear foot.

Child in Normal Mode

Figure 7D correlates time and position number with the path that was analyzed. Figures 8 and 9 show the displacement from the side and the rear, respectively, of the child's center of gravity. It can be seen in the side view that the displacement has little horizontal change indicating minimal forward and backward shifting while riding. The vertical displacement is slightly larger due to the postural adjustments required by the cambering of the vehicle, as seen in the rear view.

Figures 10 and 11 show the velocity of the center of gravity from the side and rear views respectively. Although they both reach maximum values within 10 cm/sec (3.9 inches/sec) of each other in the horizontal direction (out of a total of 19.7

nches/sec), it is can be seen that they cycle at quite different ates. The magnitudes of the vertical velocities differ ubstantially in amplitude and frequency as would have been ssumed from the displacement curves. The motion of the person hen, although cyclic, appears to be quite complex.

In Figures 12 and 13, the vertical and horizontal center of ravity accelerations viewed from the side and rear, espectively, are shown. The rear view, Figure 12, shows that he radial (horizontal) acceleration ranges between 0 and 300 m/sec/sec (9.8 feet/sec/sec or approximately 0.3g) while the ertical acceleration varies between +300 cm/sec/sec and -300 m/sec/sec.

Figure 14 shows the actual vehicle velocity measured during he excursion(s) shown in Figures 8-13, while Figure 15 shows he vehicle acceleration. It is interesting to note that the ehicular acceleration is approximately the same magnitude as the ody center of gravity acceleration. The acceleration is in hase with the body's horizontal center of gravity acceleration, ut 180° out of phase with the vertical component. A complex hree-dimensional movement is exhibited. Figures 16 and 17 show he sequence and range of movements in the form of stick figures.

Child in Braking Mode

In the braking mode, the subject had little side to side otion as viewed from the rear, so the analysis was performed nly on the side view. Figure 17A correlates time and position umber with the path traveled. Figure 18 shows that during raking the vertical position of the center of gravity changes

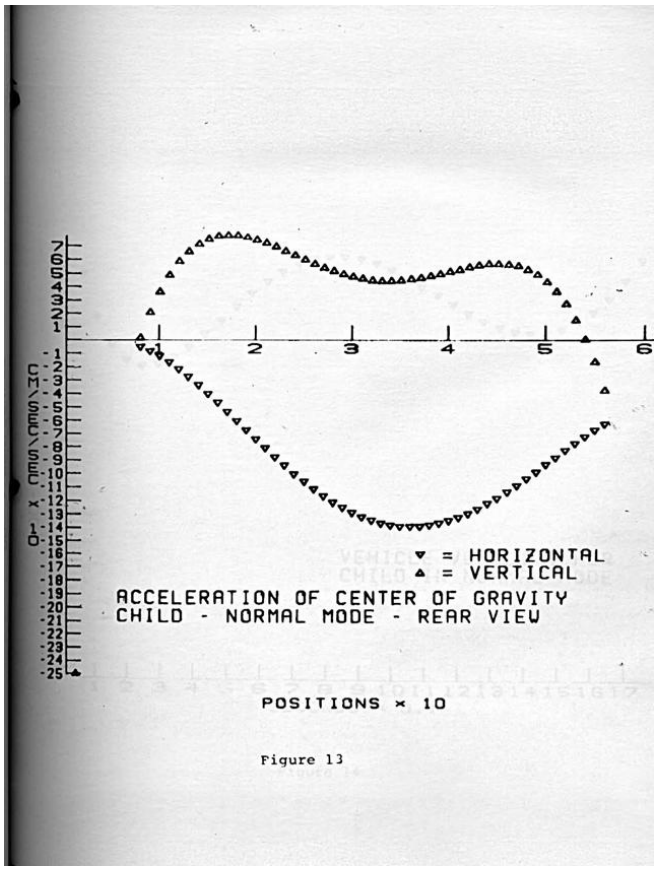

Figure 13

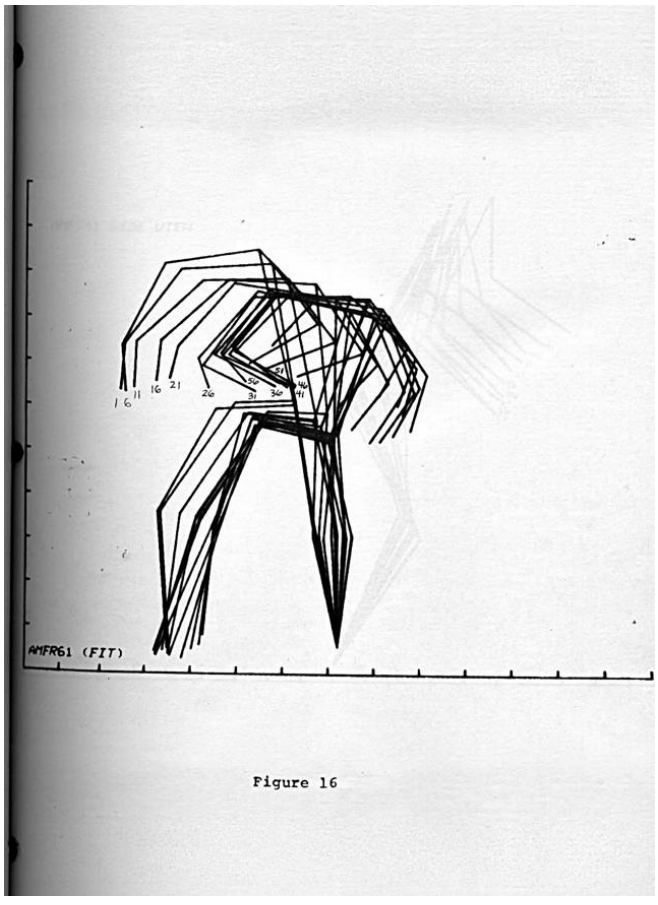

Figure 16

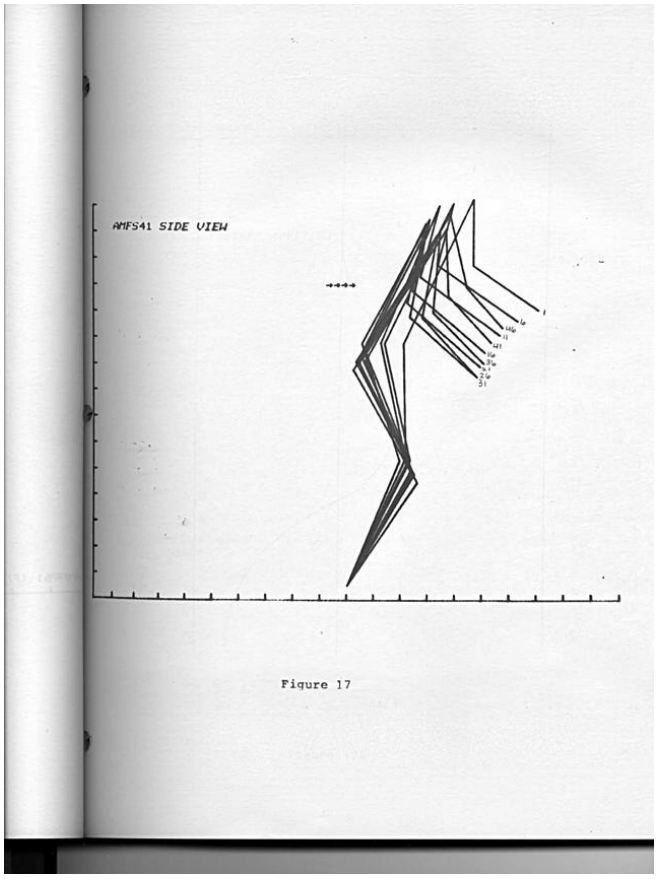

Figure 17

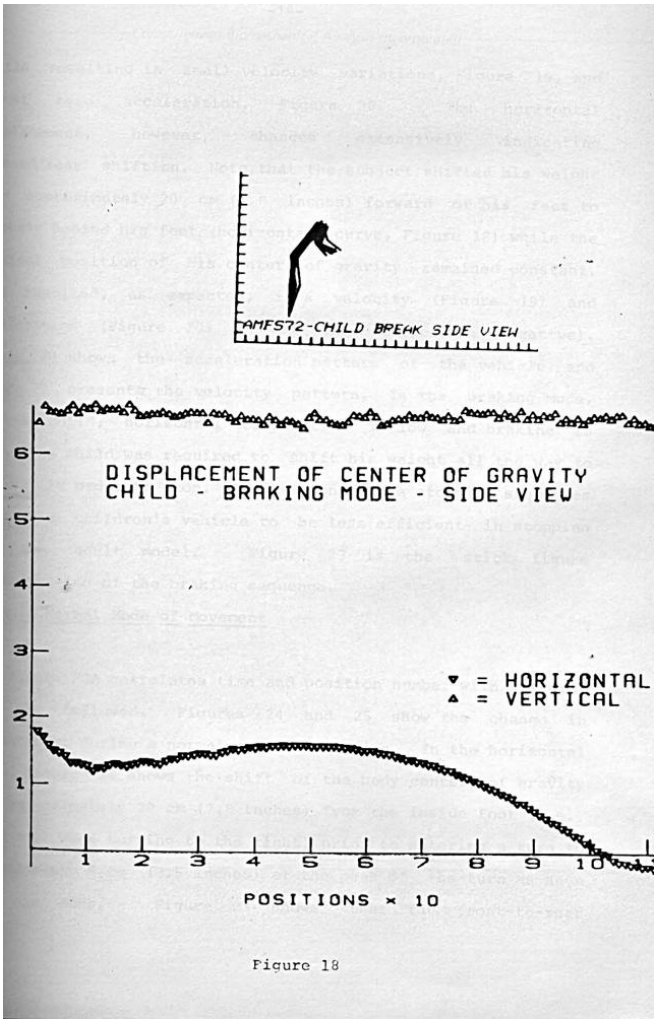

Figure 18

little resulting in small velocity variations, Figure 19, and almost zero acceleration, Figure 20. The horizontal displacement, however, changes extensively indicating forward/rear shifting. Note that the subject shifted his weight from approximately 20 cm (7.8 inches) forward of his feet to slightly behind his feet (horizontal curve, Figure 18) while the vertical position of his center of gravity remained constant. This resulted, as expected, in a velocity (Figure 19) and acceleration (Figure 20) in the rear direction (negative). Figure 21 shows the acceleration pattern of the vehicle and Figure 22 presents the velocity pattern. In the braking mode, for the child, horizontal acceleration is low and braking is slow. The child was required to shift his weight all the way to the rear in order to stop. Observation of the stopping sequences showed the children's vehicle to be less efficient in stopping than the adult model. Figure 23 is the stick figure representation of the braking sequence.

Adult in Normal Mode of Movement

Figure 23A correlates time and position number with the path that was followed. Figures 24 and 25 show the change in displacement during a normal adult excursion. In the horizontal plane, Figure 24 shows the shift of the body center of gravity from approximately 20 cm (7.8 inches) from the inside foot (i.e., right foot when turning to the right) prior to entering a turn to approximately 9 cm (3.5 inches) at the peak of the turn as seen from the rear. Figure 25 shows that the front-to-rear

displacement is approximately the same magnitude, and that the rider shifts his weight forward before entering the turn and to the rear at its peak.

When viewed from the rear (Figure 24), the rider shifts his body down slightly while beginning a turn but remains in the same position after turning. This type of motion is typical of most activities in which inertia is the driving force(e.g., ice skating).

The velocities of the body center of gravity are shown in Figure 26 and 27. When viewed from the rear, vertical position is cyclical while the horizontal position changes at a constant rate. In the side view, the opposite effect is seen with the horizontal more cyclical than the vertical. This suggests a "bobbing" motion with fairly steady side-to-side movement and a concurrent cyclical shifting front to rear. The "bobbing" is less prominent from the rear view than from the side because of the shifting. The body center of gravity velocities reach values of approximately 40 cm/sec (15.75 inches/sec), which is approximately 80% of that of the child's.

The acceleration of the center of gravity as seen from the side, Figure 29, varies at about the same rate vertically and horizontally, approximately 180' out of phase, between -100 and +250 cm/sec/sec (-3.3 to +8.2feet/sec/sec). The rear view, Figure 28, shows horizontal, or radial, accelerations of nearly constant negative (i.e., to the left in a right-hand turn) value and a cyclical vertical acceleration varying between -100 and +100 cm/sec/sec (3.3 feet/sec/sec).

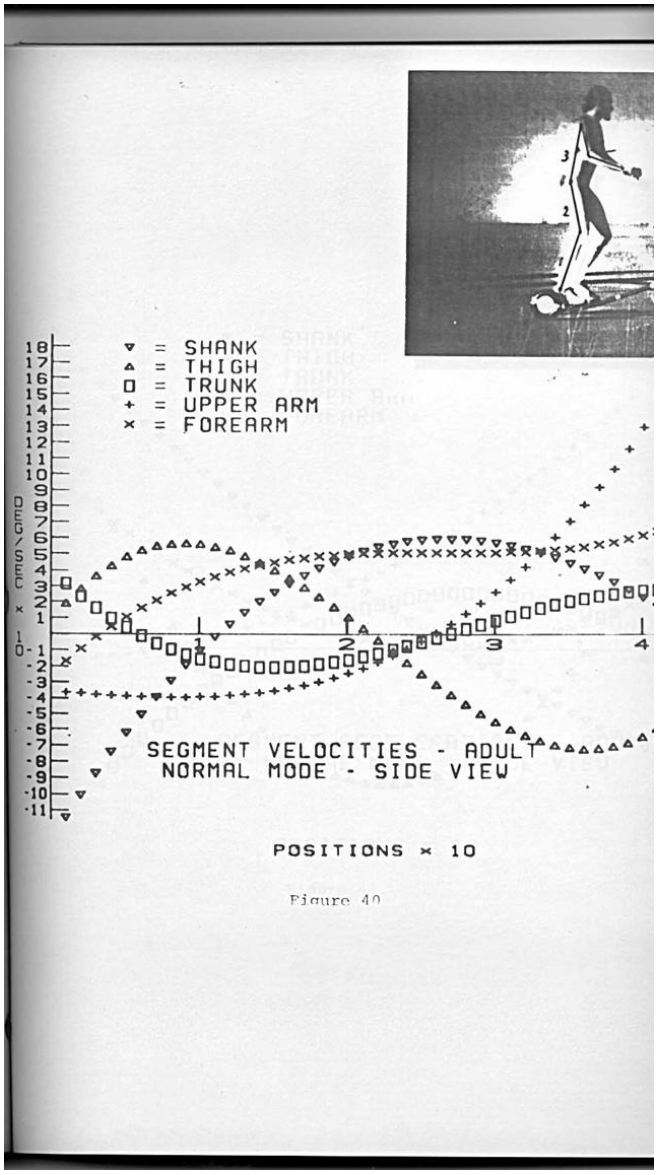

Figure 40

Relationships Among Power Units
(Power Equals Work per Unit Time)

	HORSE-POWER	KG. METERS/ MINUTE	KG. METERS/ SECOND	FOOT POUNDS/ MINUTE	FOOT POUNDS/ SECOND	WATTS	KCAL / MINUTE	KCAL / SECOND
1 HORSE-POWER	1 0	4,564 0	76.07	33,000 0	550 0	746 0	10694	0 178
1 KG.-METER/MINUTE	0 000219	1 0	0 016667	7 23	0 12 05	0 16345	0 00234	0 000039
1 FOOT POUND/MINUTE	0 000031	0 1383	0 0021	1 0	0 016667	0 0226	0 000324	0 0000054
1 WATT	0 001341	6 118	0 10197	44 236	0 7371	1 0	0 014335	0 000239
1 KCAL/MINUTE	0 093555	426 78	7 113	3096 0	51 41	69 759	1 0	0 01667

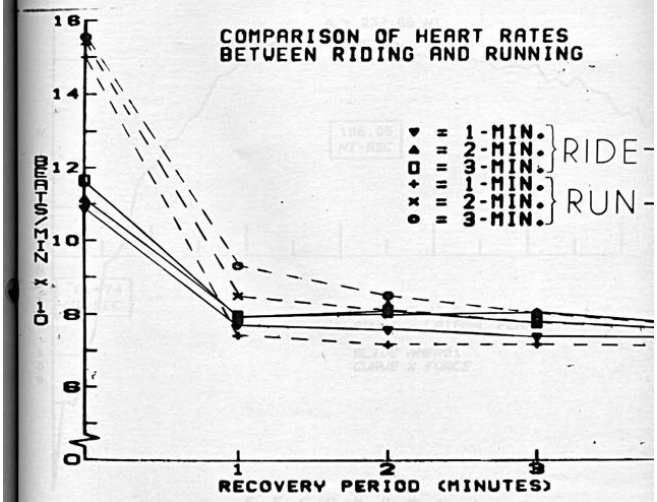

Figure 56

impact force between the rear wheel and the obstacle was made on magnetic tape for subsequent transfer to the computer for analysis.

Three typical runs were selected for the analysis with vehicular speeds between 12 and 15 mph. The forces on the rear wheel are illustrated in Table 10.

Based on the results, the maximum force that could be delivered to one leg of the body is 183.67 kg (404.08 pounds) for the adult and 63.27 kg (139.18 pounds) for the child. This force can be compared with a jump from a height of one foot. The actual force transmitted to the leg will be somewhat less than this due to the cushioning effect of the tires.

It was found that the maximum obstacle height that can pass under the vehicle frame is 1.6 inches and, thus, a height of 1.3 inches was chosen for this test to allow sufficient clearance.

The conclusion to be drawn from the bump test is that an obstacle which clears the vehicle frame may produce a vertical force which is approximately 3.0 to 5.0g (at velocites of 12 to 15 mph) on both legs and is comparable with jumping from a height of one foot.

Conclusions

1. Vehicle driving force appears to be the result of a shifting of body center of gravity in both the horizontal and vertical direction. Center of gravity shifting was due to cyclical motion of body segments

with definite phase relationships between them.

2. In braking mode for the adult, the trunk exhibited a marked angular acceleration, while all other body segments decelerated. Since results showed that a backward shift of the center of gravity was necessary for braking, it would appear that shifting of the heavier body segments, especially the trunk (55% of total body weight), resulted in most effective braking (Figure 34). In the child, a smaller shift of the horizontal center of gravity related to a lower braking force (Figure 18).

3. Heart rate comparisons revealed that traveling on the vehicle required significantly less effort (about 25% less) than jogging at the same velocity. Muscular effort (from moments computed about body joints) indicate that the effort was roughly equivalent to activities such as bowling, walking, hopping, or skipping. Furthermore, comparisons of moments of the various body joints (Figures 53A, B, C, and D) indicate that propulsion force is generated primarily by muscular action of the legs.

4. The bump test revealed that an obstacle low enough to be cleared by the vehicle frame (1.3 inches) produced a vertical force of a maximum of 5.0g which is equivalent to a vertical jump from slightly over 1 foot. This level of force is within the range of forces normally encountered in common physical activities.

Recommendations

The results of the analyses confirmed observations that the vehicles are both efficient and innovative. Some aspects of vehicular design that appear to need refinement are the difficulty in achieving rapid braking in the children's model and a tendency for the front wheel to slip sideways (especially on graveled surfaces) in the adult version. Changes in vehicle geometry might achieve a better forward-rear weight balance and help correct these problems.

The data showed the movement of the rider on the vehicle to be a complex three-dimensional harmonic one. The data already obtained, with some additional testing, could be used to provide a three-dimensional representation of the center of gravity movement. In addition, the data can be processed to yield kinematics of any part of the body during operation. A detailed mathematical analysis of the vehicle in motion, verified by high speed film measurements, would yield the changes in motion that would result from varying the stance width, handlebar length, wheel radius, tire pressure, or other physical parameters. A more comprehensive energy cost analysis (as discussed in the text) is recommended.